Collisional absorption in aluminum

D. Semkat, R. Redmer, and Th. Bornath
Universität Rostock, Institut für Physik, D–18051 Rostock, Germany
(Received 23 January 2006; published 30 June 2006)

The interaction of ultrashort laser pulses with matter is a topic of growing interest. In particular, recent developments on free-electron lasers have opened an unexplored field in which many interesting physical phenomena are to be expected. Since hydrodynamic descriptions of the interaction process need a microscopic "input," a quantum statistical theory of energy absorption by matter is required. We present a kinetic theory of collisional absorption in dense plasmas and analyze the electron-ion collision frequency in warm dense aluminum in dependence on laser frequency and temperature.

DOI: 10.1103/PhysRevE.73.066406 PACS number(s): 52.38.Dx, 52.25.Dg, 52.25.Os

I. INTRODUCTION

Due to the impressive progress in laser technology, which makes femtosecond laser pulses of very high intensity available in laboratory experiments [1–3], interaction of matter with electromagnetic fields has become a problem of current interest. In particular, there is a recent development in the direction of shorter wavelengths and higher photon energies connected with free-electron lasers (FEL). FEL projects are in progress at SLAC (Stanford) [4] and at DESY (Hamburg) [5,6]. At DESY, the vacuum ultraviolet FEL (VUV-FEL) started its operations in 2005 with a wavelength of 32 nm [7] after a test facility already demonstrated its great capacities for high-flux and time-resolved experiments at about 100 nm wavelength [8]. Perspectively, the building of an x-ray FEL is planned.

Besides the study of the fundamentals of laser-matter interaction (e.g., plasma creation, etc.), the development opens new possibilities for the diagnostics of dense strongly coupled plasmas over a broad temperature range, i.e., in the so-called warm dense matter regime. An important diagnostic tool is Thomson scattering, which has been intensely investigated both experimentally [9] and theoretically [10–12].

Attempts to investigate the laser-matter interaction by means of a hydrodynamic description require an accurate treatment of the microscopic "input." A key quantity here is the electron collision frequency that characterizes the collisional absorption and determines macroscopic parameters as the dielectric constant and, therefore, the refractive index.

A hydrodynamic description of short-pulse laser interaction with dense matter has been presented, e.g., by Eidmann *et al.* [13] for aluminum at solid-state density. In that work, the problem of determining the collision frequency over a broad temperature range is solved by interpolating between two known limiting cases, namely the Spitzer formula for the hot plasma and the electron-phonon collision frequency for the cold solid. The interpolation is done using the harmonic mean, and unphysically high values in the intermediate temperature range of 1–100 eV are cut by a plausible physical criterion. The respective collision frequency is shown in Fig. 1.

A similar treatment of laser absorption in aluminum has been presented by Fisher *et al.* [14]. There, the electron-phonon collisions are treated more rigorously, but again the Spitzer limiting case is adopted.

Thus, there is an urgent need for a theoretical investigation of the collision frequency for solid-state density matter in the range of moderate temperatures, i.e., in the warm dense matter regime. A powerful tool for such a description is given by quantum kinetic theory [15–17]. An alternative approach is molecular-dynamics simulation [17,18]. The goal of the present paper is (i) to present the theoretical background for the quantum kinetic description of collisional absorption in dense plasmas, (ii) to derive a general expression for the electron-ion collision frequency $\nu_{ei}(\omega)$ valid also for high fields, and (iii) to present some results for $\nu_{ei}(\omega)$ for dense aluminum. Concerning (i) and (ii), we follow the approach given in [15–17]. For an extension to partially ionized plasmas including bound-free transitions, see [16,19].

II. THEORETICAL BACKGROUND

A. Basic equations

In the present paper, we consider the physical phenomenon of collisional absorption, i.e., absorption due to particle scattering, a process connected with an energy transfer be-

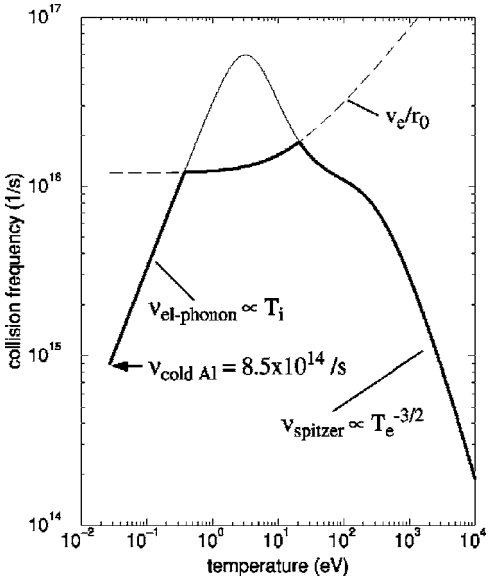

FIG. 1. Collision frequency of solid Al as a function of the temperature. The figure is taken from Ref. [13].

tween plasma and field. This quantity is determined by the electric current density $\mathbf{j}(\mathbf{E})$ due to the field $\mathbf{E}$,

$$\frac{dW^{\mathrm{kin}}}{dt} + \frac{dW^{\mathrm{pot}}}{dt} = \mathbf{j}\cdot\mathbf{E}, \tag{1}$$

i.e., the change of the total energy of the system of particles is equal to $\mathbf{j}\cdot\mathbf{E}$, which is in turn the energy loss of the electromagnetic field due to Poynting's theorem.

A central quantity is, therefore, the electrical current density defined by

$$\mathbf{j}(t) = \sum_a \mathbf{j}_a(t) = \sum_a \int \frac{d^3p}{(2\pi\hbar)^3}\frac{e_a\mathbf{p}_a}{m_a} f_a(p_a,t), \tag{2}$$

where $f_a(p_a,t)$ is the single-particle gauge invariant Wigner function of the species a ($a=e,i$ for electrons and ions, respectively). For the determination of f_a, we start from the kinetic equation [20]

$$\left\{\frac{\partial}{\partial t} + e_a\mathbf{E}(t)\cdot\nabla_{k_a}\right\} f_a(\mathbf{k}_a,t) = I_a(\mathbf{k}_a,t), \tag{3}$$

where the collision integral is given by ($\mathcal{V}$ being the volume and V_{ab} the interaction potential)

$$I_a(\mathbf{p},t) = \sum_b \frac{1}{\mathcal{V}}\int \frac{d^3q\,d^3p_1\,d^3p_2}{(2\pi\hbar)^6}[\delta(\mathbf{p}-\mathbf{p}_1-\mathbf{q}) - \delta(\mathbf{p}-\mathbf{p}_1)] \times V_{ab}(\mathbf{q})F_{ab}(\mathbf{p}_1,\mathbf{p}_1+\mathbf{q},\mathbf{p}_2,\mathbf{p}_2-\mathbf{q},t). \tag{4}$$

The two-particle density matrix is connected with the correlation function of density fluctuations by [15,21]

$$F_{ab}(t) = (i\hbar)^2 g_a^<(1t,1't)g_b^<(2t,2't) + (i\hbar)L_{ab}^<(11't,22't)\ (a\neq b), \tag{5}$$

where the latter function is defined by

$$(i\hbar)L_{ab}^<(11't,22't') = \langle \delta\hat{\rho}_b(22't')\delta\hat{\rho}_a(11't)\rangle \tag{6}$$

with $\delta\hat{\rho}_a(11't) = \Psi_a^+(1',t)\Psi_a(1,t) - \langle\Psi_a^+(1',t)\Psi_a(1,t)\rangle$.

The balance equation for the electrical current density follows from Eq. (3) [15]:

$$\frac{d}{dt}\mathbf{j}_a(t) - n_a\frac{e_a^2}{m_a}\mathbf{E}(t) = \sum_{b\neq a}\int\frac{d^3q}{(2\pi\hbar)^3}\frac{e_a\mathbf{q}}{m_a}V_{ab}(q)L_{ba}^<(\mathbf{q};t,t). \tag{7}$$

The correlation function $L_{ba}^<$ follows from its equation of motion defined on the Keldysh contour (for brevity all arguments are suppressed),

$$L_{ab} = \Pi_{ab} + \sum_{c,d}\Pi_{ac}V_{cd}L_{db}. \tag{8}$$

In a plasma in a strong laser field, the coupling between species with different charges can be considered to be weak, whereas the coupling between particles with equal charges is not affected by the field. Then the polarization functions Π_{ab} can be adopted to be diagonal, $\Pi_{ab}=\delta_{ab}\Pi_a$, and an approximation in lowest order of V_{ie} is appropriate. We find [21]

$$L_{ei}^{\gtrless}(\mathbf{q};t,t') = \int d\bar{t}\,[\mathcal{L}_{ee}^{\gtrless}(\mathbf{q};t,\bar{t})V_{ei}(q)\mathcal{L}_{ii}^A(\mathbf{q};\bar{t},t') + \mathcal{L}_{ee}^R(\mathbf{q};t,\bar{t})V_{ei}(q)\mathcal{L}_{ii}^{\gtrless}(\mathbf{q};\bar{t},t')]. \tag{9}$$

Here the functions $\mathcal{L}_{aa}^{R/A}$ and $\mathcal{L}_{aa}^{\gtrless}$ are density response functions and correlation functions of density fluctuations, respectively, of the electron and ion subsystems with $\mathcal{L}_{aa} = \Pi_a + \Pi_a V_{aa}\mathcal{L}_{aa}$.

For the electron current (7) it follows that

$$\frac{\mathrm{d}}{\mathrm{d}t}\mathbf{j}_e(t) - n_e\frac{e_e^2}{m_e}\mathbf{E}(t) = \mathrm{Re}\int\frac{d^3q}{(2\pi\hbar)^3}\frac{e_e\mathbf{q}}{m_e\hbar}V_{ei}(q)2\pi i\int_{t_0}^t d\bar{t}\,[S_{ee}(\mathbf{q};t,\bar{t})V_{ei}(q) \times\mathcal{L}_{ii}^A(\mathbf{q};\bar{t},t) + \mathcal{L}_{ee}^R(\mathbf{q};t,\bar{t})V_{ei}(q)S_{ii}(\mathbf{q};\bar{t},t)], \tag{10}$$

where we have introduced the dynamical structure factor

$$2\pi S_{aa}(\mathbf{q};t,\bar{t}) = \frac{i\hbar}{2}[\mathcal{L}_{aa}^>(\mathbf{q};t,\bar{t}) + \mathcal{L}_{aa}^<(\mathbf{q};t,\bar{t})]. \tag{11}$$

The functions in the collision term depend on the current and the electrical field. This dependence can be made explicit if one assumes that each subsystem (electrons and ions) is in local equilibrium with a temperature T_a with respect to a coordinate frame moving with the mean velocity $\mathbf{u}_a(t)$ [22,23]. The transformation between such a coordinate system and a system at rest is given by $\tilde{\mathbf{r}} = \mathbf{r} - \int_{t_0}^t d\bar{t}\,\mathbf{u}_a(\bar{t})$. The Fourier transforms in the two coordinate systems are connected by

$$\mathcal{L}_{aa}(\mathbf{q},t_1t_2) = e^{-(i/\hbar)\mathbf{q}\cdot\int_{t_2}^{t_1}d\bar{t}\,\mathbf{u}_a(\bar{t})}\tilde{\mathcal{L}}_{aa}(\mathbf{q},t_1-t_2), \tag{12}$$

where $\tilde{\mathcal{L}}_{aa}$ denotes the local equilibrium function depending on the time difference only. One gets (omitting the tilde from now on)

$$\frac{\mathrm{d}}{\mathrm{d}t}\mathbf{j}(t) = \varepsilon_0\omega_p^2\mathbf{E}(t) - \mathrm{Re}\int\frac{d^3q}{(2\pi\hbar)^3}\mathbf{q}\frac{e_e}{m_e}V_{ie}(q)\frac{2\pi}{i\hbar} \times\int_{t_0}^t d\bar{t}\,[S_{ee}(\mathbf{q};t-\bar{t})V_{ei}(q)\mathcal{L}_{ii}^A(\mathbf{q};\bar{t}-t) + \mathcal{L}_{ee}^R(\mathbf{q};t-\bar{t})V_{ei}(q)S_{ii}(\mathbf{q};\bar{t}-t)] \times\exp\left\{-\frac{i}{\hbar}\frac{1}{n_ee_e}\mathbf{q}\cdot\int_{\bar{t}}^t d\bar{t}_1\mathbf{j}(\bar{t}_1)\right\} \tag{13}$$

Thus, the source term in the current balance equation depends on the current itself in a nonlinear way. In order to proceed with the analysis, we will consider weak fields and strong high-frequency fields as limiting cases.

B. Weak fields

In the case of weak fields, we can expand the exponential function and get a term linear in $\mathbf{j}$. Adopting a harmonic time dependence of the electric field, we have for the current $\mathbf{j}(t) = \mathbf{j}(\omega)e^{-i\omega t} + \mathbf{j}^*(\omega)e^{i\omega t}$ and get from the above equation

$$\mathbf{j}(\omega) = \frac{\varepsilon_0 \omega_p^2}{-i\omega + \nu_{ei}(\omega)} \mathbf{E}(\omega), \tag{14}$$

which is a generalized Drude equation. The complex electron-ion collision frequency ν_{ei},

$$\nu_{ei}(\omega) = i \frac{n_i e_i^2}{n_e m_e \hbar^2} \int \frac{d^3q}{(2\pi\hbar)^3} \frac{1}{\omega} (\mathbf{q}\cdot\mathbf{n})^2 S_{ii}(q) V(q) [\varepsilon_{ee}^{-1}(\mathbf{q};\omega) - \varepsilon_{ee}^{-1}(\mathbf{q};0)], \tag{15}$$

is defined via the dielectric function of the electron subsystem,

$$\varepsilon_{ee}^{-1}(\mathbf{q};\omega) = 1 + e^2 V(q) \mathcal{L}_{ee}(\mathbf{q};\omega), \tag{16}$$

and the static ion-ion structure factor $S_{ii}(q)$. Using for ε_{ee}^{-1} the random phase approximation (RPA), this is the well-known expression first given by Bekefi [24] and later, for instance, by Reinholz *et al.* [25]. One gets immediately the dynamical conductivity

$$\sigma(\omega) = \frac{\varepsilon_0 \omega_{pl}^2}{-i\omega + \nu_{ei}(\omega)}. \tag{17}$$

In the limit of high frequencies, one gets $\sigma(\omega) \approx (\varepsilon_0 \omega_{pl}^2/\omega^2) \times [i\omega + \nu_{ei}(\omega)]$ [26], and the averaged absorbed energy is given by

$$\begin{aligned} \langle \mathbf{j}\cdot\mathbf{E} \rangle &\equiv \frac{1}{T} \int_{t-T}^{T} dt' \mathbf{j}(t')\cdot\mathbf{E}(t') \\ &= \frac{\omega_{pl}^2}{\omega^2} \mathrm{Re}\ \nu_{ei}(\omega) \frac{\varepsilon_0 \mathbf{E}_0^2}{2} \\ &= \frac{\omega_{pl}^2}{\omega^2} \mathrm{Re}\ \nu_{ei}(\omega) \langle \varepsilon_0 \mathbf{E}^2 \rangle. \end{aligned} \tag{18}$$

C. Strong high-frequency fields

In the case of strong fields, the dependence on the electric field has an exponential form and causes, therefore, nonlinear effects like multiphoton absorption and the occurrence of higher harmonics in the current. We can apply on the right-hand side of Eq. (13)

$$\mathbf{j} \approx \mathbf{j}^0 = \sum_a \frac{e_a^2 n_a}{m_a} \int_{t_0}^{t} \mathrm{d}t' \mathbf{E}(t'), \tag{19}$$

i.e., collisions are regarded as small perturbations compared to the strong field, which corresponds to the so-called Silin ansatz [27]. For a harmonic electric field, $\mathbf{E} = \mathbf{E}_0 \cos \omega t$, the exponential factor in Eq. (13) can then be expanded into a Fourier series. For the current balance, it follows that

$$\begin{aligned} \frac{d}{dt}\mathbf{j}_e(t) - n_e \frac{e_e^2}{m_e} \mathbf{E}(t) = \mathrm{Re} \int \frac{d^3q}{(2\pi\hbar)^3} \frac{2\pi e_e \mathbf{q}}{m_e \hbar} V_{ei}^2(q) \\ \times \sum_m \sum_n (-i)^{m+1} J_n\left(\frac{\mathbf{q}\cdot\mathbf{v}_0}{\hbar\omega}\right) \\ \times J_{n-m}\left(\frac{\mathbf{q}\cdot\mathbf{v}_0}{\hbar\omega}\right) e^{im\omega t} \\ \times \int_{-\infty}^{\infty} \frac{d\bar{\omega}}{2\pi} [S_{ee}(\mathbf{q};\bar{\omega} - n\omega) \mathcal{L}_{ii}^A(\mathbf{q};\bar{\omega}) \\ + \mathcal{L}_{ee}^R(\mathbf{q};\bar{\omega} - n\omega) S_{ii}(\mathbf{q};\bar{\omega})] \end{aligned} \tag{20}$$

with the one-component structure factors and response functions S_{aa} and $\mathcal{L}_{aa}$, respectively [15,21]. We will assume in the rest of this section that the subsystems are in local thermodynamic equilibrium with temperatures T_e and T_i, respectively (the influence of non-Maxwellian distribution functions was considered in [28], and a numerical solution of a kinetic equation for a strong laser field was performed in [29]). J_l is the Bessel function of lth order and $\mathbf{v}_0 = (e_e/m_e)\mathbf{E}_0/\omega$ is the quiver velocity. Note that there is the same functional dependence of the electron and ion contributions to the screening in Eq. (20). The ion functions, however, are localized in the low-frequency region, i.e., for a high-frequency electric field, $\bar{\omega}$ can be neglected in comparison with $n\omega$. In this case, the first term in the brackets in Eq. (20) vanishes because $\int d\bar{\omega} \mathcal{L}_{ii}^A(\mathbf{q};\bar{\omega}) = 0$, and for the current it follows that

$$\begin{aligned} \mathbf{j}_e(t) - \int_{-\infty}^{t} d\bar{t} \frac{n_e e_e^2}{m_e} \mathbf{E}(\bar{t}) = \mathrm{Re} \int \frac{d^3q}{(2\pi\hbar)^3} \sum_m \sum_n \frac{e_e}{m_e} \frac{\mathbf{q}}{m\hbar\omega} V_{ei}^2(q) \\ \times (-i)^{m+2} e^{im\omega t} J_n\left(\frac{\mathbf{q}\cdot\mathbf{v}_0}{\hbar\omega}\right) \\ \times J_{n-m}\left(\frac{\mathbf{q}\cdot\mathbf{v}_0}{\hbar\omega}\right) \mathcal{L}_{ee}^R(\mathbf{q};-n\omega) n_i S_{ii}(\mathbf{q}). \end{aligned} \tag{21}$$

The screening by the ions is accounted for by the static structure factor $S_{ii}(\mathbf{q})$ defined by

$$S_{ii}(\mathbf{q}) \equiv \frac{1}{n_i} \int d\bar{\omega} S_{ii}(\mathbf{q},\bar{\omega}) = 1 + n_i \int d^3r [g_{ii}(\mathbf{r}) - 1] e^{-(i/\hbar)\mathbf{q}\cdot\mathbf{r}}, \tag{22}$$

where $g_{ii}(\mathbf{r})$ is the pair distribution function. $\mathcal{L}_{ee}^R$ is the exact density response function of the electron subsystem which can be approximated using local field corrections [21].

The Fourier coefficients of the current can be identified easily from Eq. (21). Only the odd harmonics are allowed due to the symmetry of the interaction, cf. [30]. The cycle averaged dissipation of energy is given by

$$\begin{aligned} \langle \mathbf{j}\cdot\mathbf{E} \rangle = n_i \int \frac{d^3q}{(2\pi\hbar)^3} \frac{V_{ei}^2(q)}{V_{ee}(q)} S_{ii}(\mathbf{q}, T_i) \\ \times \sum_{n=-\infty}^{\infty} n\omega J_n^2\left(\frac{\mathbf{q}\cdot\mathbf{v}_0}{\hbar\omega}\right) \mathrm{Im}\ \varepsilon_{ee}^{-1}(\mathbf{q}, -n\omega, T_e). \end{aligned} \tag{23}$$

Then we get for the collision frequency

$$\mathrm{Re}\,\nu_{ei}(\omega) = \frac{4n_i}{\varepsilon_0 E_0^2}\frac{\omega^2}{\omega_{pl}^2}\int \frac{d^3q}{(2\pi\hbar)^3}\frac{V_{ei}^2(q)}{V_{ee}(q)}S_{ii}(\mathbf{q},T_i) \times\sum_{n=1}^{\infty} n\omega J_n^2\left(\frac{\mathbf{q}\cdot\mathbf{v}_0}{\hbar\omega}\right)\mathrm{Im}\,\varepsilon_{ee}^{-1}(\mathbf{q},-n\omega,T_e), \tag{24}$$

where V_{ei} is the electron-ion interaction potential. This formula contains interesting many-particle and field effects: (i) The influence of the field manifests itself in the sum over n reflecting multiphoton processes. While any n-photon process is determined by the inverse dielectric function at the frequency $n\omega$, the amplitude is given by the square of the Bessel function of order n. (ii) Dynamical screening and correlations in the electron subsystem are described by the dielectric function ε_{ee}. (iii) The ionic structure factor S_{ii} contains the correlations of the ion subsystem.

III. NUMERICAL EVALUATION

In order to evaluate Eq. (24), the quantities entering the right-hand side have to be specified. We apply the following approximations:

(i) The dielectric function of the electrons ε_{ee} is calculated in the random phase approximation (RPA),

$$\mathrm{Im}\,\varepsilon_{ee}^{-1}(\mathbf{q},\omega) = -\frac{\mathrm{Im}\,\varepsilon_{ee}(\mathbf{q},\omega)}{|\varepsilon_{ee}(\mathbf{q},\omega)|^2} \tag{25}$$

with

$$\mathrm{Im}\,\varepsilon_{ee}(\mathbf{q},\omega) = \frac{e^2}{\varepsilon_0}\frac{\hbar^2}{q^2}\int \frac{d^3q}{(2\pi\hbar)^3}\pi\delta(\hbar\omega + E(\mathbf{p}) - E(\mathbf{p}+\mathbf{q})) \times\{f(\mathbf{p}) - f(\mathbf{p}+\mathbf{q})\}, \tag{26}$$

$$\mathrm{Re}\,\varepsilon_{ee}(\mathbf{q},\omega) = 1 + \frac{e^2}{\varepsilon_0}\frac{\hbar^2}{q^2}\mathcal{P}\int \frac{d^3q}{(2\pi\hbar)^3}\frac{f(\mathbf{p}) - f(\mathbf{p}+\mathbf{q})}{\hbar\omega + E(\mathbf{p}) - E(\mathbf{p}+\mathbf{q})}. \tag{27}$$

(ii) The electron-ion interaction is in general given by the interaction of a point charge (electron) with a charge cloud (ion). Its determination is a complicated task for many-electron ions. We, therefore, replace it in a first approximation by the Coulomb interaction, which is justified for not too high densities. Then we get

$$\frac{V_{ei}^2(q)}{V_{ee}(q)} = Z^2 V_{ee}(q) = \frac{Z^2e^2}{4\pi\epsilon_0}\frac{\hbar^2}{q^2}. \tag{28}$$

(iii) The static ionic structure factor is given by Eq. (22), where the pair distribution function g obeys the Ornstein-Zernike equation,

$$h(\mathbf{r}) = g(\mathbf{r}) - 1 = c(\mathbf{r}) + n\int d^3r' c(|\mathbf{r}-\mathbf{r}'|)h(\mathbf{r}'). \tag{29}$$

The latter equation can be solved numerically in the hypernetted chain (HNC) approximation,

$$g(\mathbf{r}) = \exp\{-\beta V(\mathbf{r}) + h(\mathbf{r}) - c(\mathbf{r})\}. \tag{30}$$

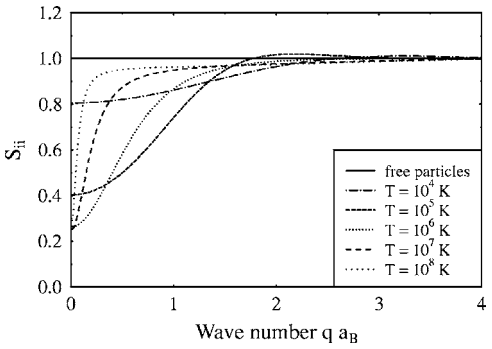

FIG. 2. Ion-ion structure factor for aluminum at solid-state density, $\rho=2.7$ g/cm^3 (corresponding to an ion density of $n_i=6\times10^{22}$ cm^{-3}) from HNC calculations for several temperatures. The effective ion radius is chosen to be $r_0=0.054$ nm $=1.05a_B$ (the radius of Al^{3+} ions in a crystal [31]).

Figure 2 shows results for S_{ii} obtained by HNC calculations in comparison with the free-particle case $S\equiv1$.

A. Weak fields

In the case of weak fields, the amplitudes for higher-order photon processes are small and can be neglected compared to that of the single-photon process. Furthermore, in the series expansion of the Bessel function (which is here, in principle, an expansion in powers of the field), the first term dominates. Thus, we can replace in Eq. (24)

$$\sum_{n=1}^{\infty} n\omega J_n^2\left(\frac{\mathbf{q}\cdot\mathbf{v}_0}{\hbar\omega}\right)\mathrm{Im}\,\varepsilon_{ee}^{-1}(\mathbf{q},-n\omega,T_e) \approx \omega J_1^2\left(\frac{\mathbf{q}\cdot\mathbf{v}_0}{\hbar\omega}\right)\mathrm{Im}\,\varepsilon_{ee}^{-1}(\mathbf{q},-\omega,T_e) \approx \frac{\omega}{4}\left(\frac{\mathbf{q}\cdot\mathbf{v}_0}{\hbar\omega}\right)^2\mathrm{Im}\,\varepsilon_{ee}^{-1}(\mathbf{q},-\omega,T_e). \tag{31}$$

For the collision frequency, we obtain

$$\mathrm{Re}\,\nu_{ei}(\omega) = \frac{Z^2e^4n_i}{6\pi^2\varepsilon_0^2m_e^2\hbar^3\omega^3}\frac{\omega^2}{\omega_{pl}^2}\int_0^{\infty} dqq^2S_{ii}(\mathbf{q},T_i) \times\mathrm{Im}\,\varepsilon_{ee}^{-1}(\mathbf{q},-\omega,T_e). \tag{32}$$

We calculate the collision frequency for aluminum at solid-state density, $n_i=6\times10^{22}$ cm^{-3}. The charge state of the ions is assumed to be $Z=3$. Figure 3 shows $\mathrm{Re}\nu_{ei}$ as a function of the laser frequency with and without inclusion of the ionic structure factor. The electron temperature is 10^5 K. In the case of uncorrelated ions ($S_{ii}=1$), the collision frequency exhibits the well-known behavior with a plateau for small frequencies and a typical resonance peak at $\omega=\omega_{\mathrm{pl}}$ [25,30]. Qualitatively, the behavior is the same if the structure factor is taken into account. However, the plateau height is reduced significantly and the resonance is much less pronounced.

In Fig. 4, the temperature dependence of the collision frequency is shown. Again, the HNC result for the ionic structure factor is compared with the uncorrelated case. The figure shows the situation of an isothermal plasma, $T_i=T_e$. A two-

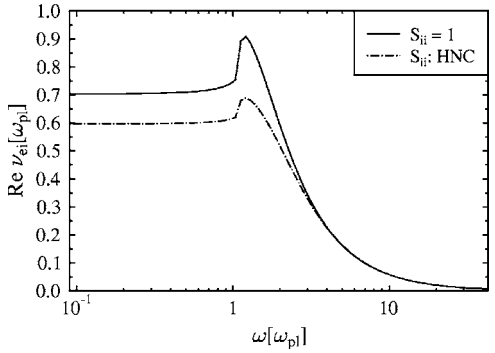

FIG. 3. Real part of the electron-ion collision frequency vs laser frequency for aluminum. System parameters: see Fig. 2. The result using the HNC static ion-ion structure factor is compared with the free-particle case.

temperature plasma with $T_e > T_i$ is the experimentally more realistic situation [32,33], for a theoretical analysis see, e.g., [34,35]. However, the quantitative influence on the collision frequency is small. Two different laser wavelengths have been assumed: (a) an optical laser with $\lambda = 800$ nm, and (b) a VUV-FEL with $\lambda = 32$ nm (corresponding to the current operation of the VUV-FEL at DESY, Hamburg). Obviously, the structure factor has a significant quantitative influence only at lower ion temperatures, while it does not change the result qualitatively, cf. also calculations for hydrogen in [17].

The deviation from the Spitzer limiting case at high temperatures can be overcome by taking into account higher moments of the distribution function. This has been analyzed by Reinholz *et al.* [25]. They derived a frequency-dependent renormalization factor that describes the effects of higher moments. However, at lower temperatures (higher degeneracy) a single-moment approximation is sufficient.

For low temperatures, $T \lesssim 10^4$ K, our model is, of course, not sufficient. At lower temperatures, the electron–phonon interaction is the dominating absorption process and, therefore, gives the main contribution to the collision frequency. This will be discussed later.

B. Strong fields

In the case of stronger fields, the multiphoton processes [cf. Eq. (24)] have finite amplitudes that cannot be neglected compared to that of the single-photon process. The collision frequency takes the form

$$\mathrm{Re}\,\nu_{ei}(\omega) = \frac{Z^2 e^2 n_i}{\pi^2 \varepsilon_0^2 \hbar\, E_0^2} \frac{\omega^2}{\omega_{\mathrm{pl}}^2} \int_0^\infty dq S_{ii}(\mathbf{q}, T_i) \times \sum_{n=1}^{\infty} n\omega\, \mathrm{Im}\varepsilon_{ee}^{-1}(\mathbf{q}, -n\omega, T_e) \int_{-1}^{1} dz J_n^2\left(\frac{eE_0 q}{m_e \hbar\, \omega^2} z\right). \tag{33}$$

Evidently, the numerical effort is now much greater than in the weak-field case. One additional integral has to be solved, the dielectric function has to be computed n times (at the frequencies $n\omega$), and the summation over n has to be performed.

The Bessel functions show rapid oscillations for large arguments. Therefore, we use the following asymptotic expression for $I_n(a) = \int_0^1 dz J_n^2(az)$ in the limit of large a (i.e., strong field, large q / small ω) [22,36]:

$$I_n(a) = \frac{1}{\pi a} \mathrm{arcosh}\left(\frac{a}{n}\right), \quad a \geq n. \tag{34}$$

On the other hand, for small a (weak field, small q / large ω), from the series expansion of the Bessel function it follows that

$$I_n(a) = \frac{1}{2n+1}\left(\frac{a^n}{2^n n!}\right)^2. \tag{35}$$

Figure 5 shows the real part of the dynamic collision frequency in dependence on the laser frequency for several field strengths in comparison with the linear response case. We see that, up to fields corresponding to an intensity of $I \approx 10^{12}$ W/cm^2, essentially the linear response result is repro-

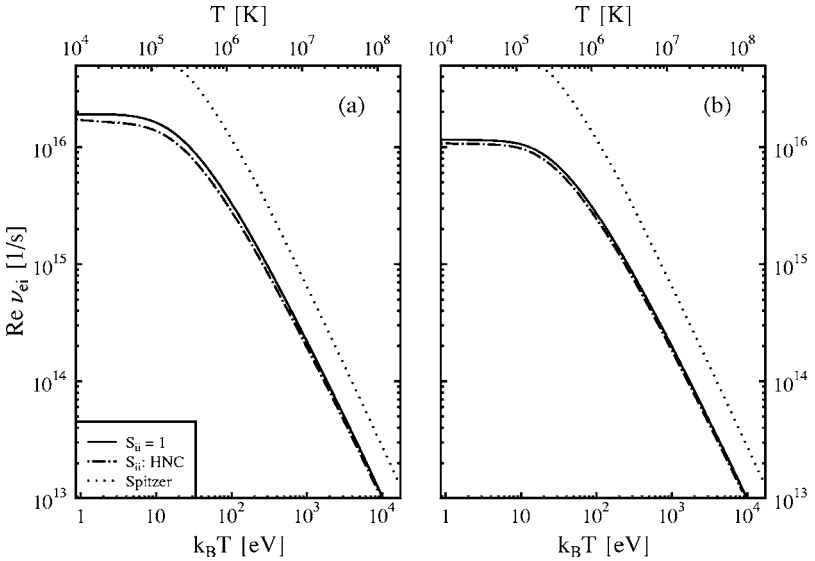

FIG. 4. Real part of the electron-ion collision frequency vs electron temperature for aluminum ($n_i = 6 \times 10^{22}$ cm^{-3}, $T_i = T_e$) for two different laser wavelengths: (a) $\lambda = 800$ nm, (b) $\lambda = 32$ nm. The HNC result for S_{ii} is compared with the free-particle case. In addition, the limiting case for high T (Spitzer formula) is shown.

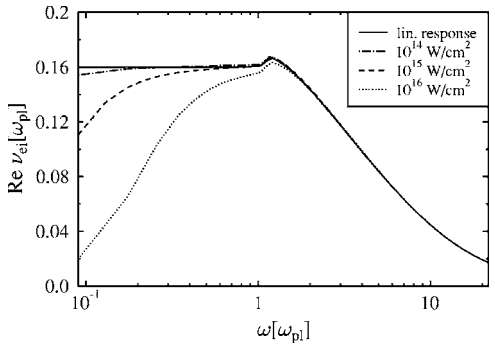

FIG. 5. Real part of the electron-ion collision frequency vs laser frequency for aluminum at solid-state density and a temperature of $T=10^6$ K for several laser intensities.

duced. Only for intensities $I \gtrsim 10^{14}$ W/cm^2 do deviations from the plateau behavior at $\omega < \omega_{\mathrm{pl}}$ occur, i.e., Reν_{ei} drops significantly for small frequencies.

The behavior of the collision frequency in dependence on the temperature is shown in Fig. 6 for two different laser wavelengths: 800 nm (a) and 32 nm (b). We again point out that Reν_{ei} can be described by the linear response case up to rather high fields. In the case of the optical laser with $\lambda = 800$ nm, deviations from the weak-field behavior occur at $I \gtrsim 10^{14}$ W/cm^2. For the VUV-FEL ($\lambda = 32$ nm), this limit lies even at $I \approx 10^{17}$ W/cm^2 (for comparison: the atomic field strength, i.e., the field of the proton at $1a_B$, corresponds to $I \approx 3.5 \times 10^{16}$ W/cm^2). At high temperatures, all curves agree with the weak-field result.

In order to give a quantitative measure for the strength of the field, it is convenient to consider the ratio of the quiver velocity v_0 to the thermal velocity v_{th}. Since $v_0 \sim E_0/\omega$ and $v_{\mathrm{th}} \sim \sqrt{T}$, the field influence increases with decreasing temperature and frequency, which is obvious in Figs. 5 and 6.

C. Electron-phonon collisions

In order to compare our results with those obtained in [13,14], we still have to include the contribution of the electron-phonon interaction to the dynamic collision frequency. This contribution dominates at low temperatures, i.e., in the solid state.

Eidmann *et al.* use a formula derived in [37] which for the cold solid reads [Eq. (3) of Ref. [13]]

$$\nu_{e\text{-ph}} \approx 2k_s \frac{e^2 k_B T_i}{\hbar^2 v_F}, \tag{36}$$

i.e., $\nu_{e\text{-ph}} \sim T_i$. Here, v_F is the Fermi velocity and k_s is a constant used to fit $\nu_{e\text{-ph}}$ to the value following from the measured reflectivity of Al at room temperature. The fit yields $k_s = 9.4$.

On the other hand, Fisher *et al.* [14] apply a more sophisticated theory to investigate the electron-phonon collision frequency [38]. The result of their calculations [Eq. (16) of Ref. [14]] exhibits some numerical prefactors that were fitted to experimental dc resistivity data given in [39].

In Fig. 7, we show the dynamic collision frequency over a broad temperature range. From our results presented above, we selected Reν_{ei} for a laser wavelength of $\lambda = 800$ nm in the weak field case. Furthermore, curves for $\nu_{e\text{-ph}}$ according to Eq. (36) above and to Eq. (16) of Ref. [14], respectively, are presented. Obviously, both curves agree concerning the proportionality $\nu_{e\text{-ph}} \sim T_i$, however the slope is different. This difference is apparently connected with the choice of experimental data to fit the numerical prefactors. Note that, in Ref. [14], the case of a constant ion temperature is considered while we apply their formula for an isothermal plasma.

The phonon picture is of course not well suited for temperatures exceeding the melting temperature of about 1000 K, however it can serve as a guide for the principal behavior of the collision frequency up to about 10000 K. The dashed line represents the upper limit used as cutoff criterion in [13]. Above this line, the electron mean free path is smaller than the mean interionic distance, $\lambda_e < r_0$ [i.e., $\nu > v_e/r_0$ with the characteristic electron velocity $v_e = (v_F^2 + k_B T_e/m_e)^{1/2}$]. Of course, this criterion gives only a qualitative measure, but it agrees with our result within a factor <2.

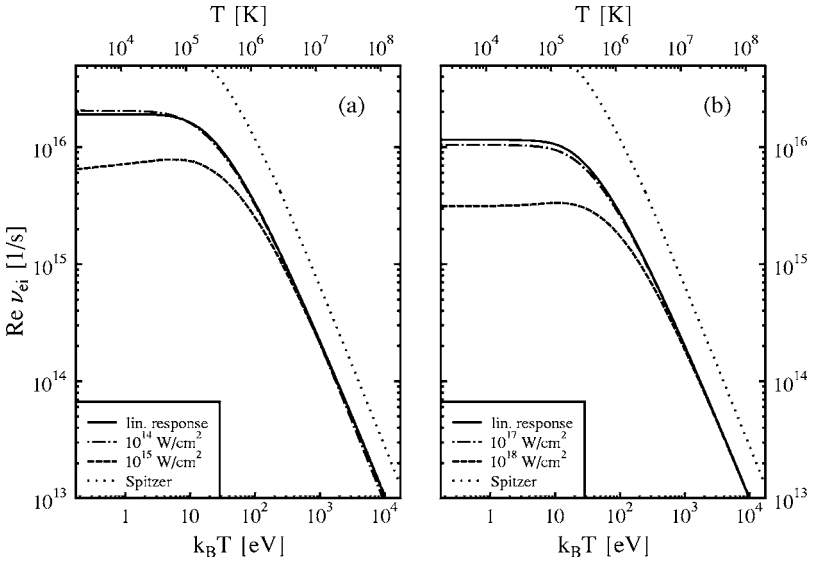

FIG. 6. Real part of the electron-ion collision frequency vs electron temperature for aluminum, $T_i = T_e$, for two different laser wavelengths: (a) $\lambda = 800$ nm, (b) $\lambda = 32$ nm, and several laser intensities. In addition, the limiting case for high T (Spitzer formula) is shown.

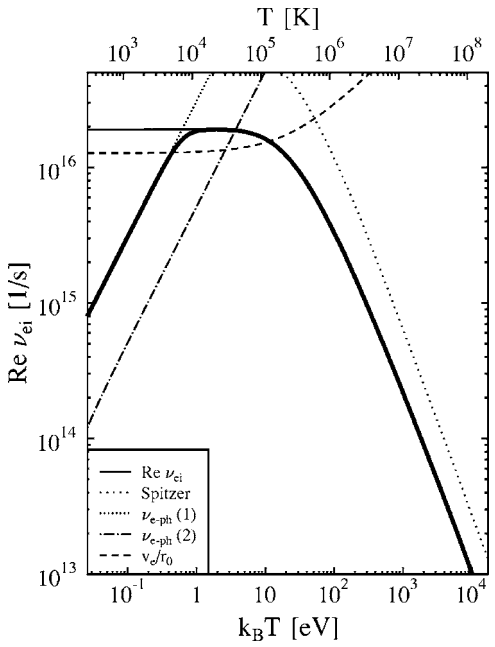

FIG. 7. Dynamic collision frequency vs electron temperature for aluminum, $T_i=T_e$. The narrow-dotted line denotes $\nu_{e\text{-ph}}$ according to Eq. (36), the dash-dotted line corresponds to Eq. (16) of Ref. [14]. The thick solid line denotes a connection of $\nu_{e\text{-ph}}$ (36) and Reν_{ei} (33).

In order to obtain a single curve for the collision frequency over the whole temperature range, a smooth connection of the results for ν_{ei} and $\nu_{e\text{-ph}}$ via the fourth-order power mean can be used that yields the thick solid curve in Fig. 7. This should be justified by the fact that the curves cross each other in a temperature region where the validity of both is, in principle, still assured.

IV. CONCLUSIONS AND OUTLOOK

In this paper, we have presented a theoretical scheme for the quantum kinetic description of collisional absorption in dense plasmas. A general expression for the electron-ion collision frequency $\nu_{ei}(\omega)$ valid for arbitrary field strengths (in the nonrelativistic domain) has been derived and discussed both in the weak-field (linear response) and high-field regime. Numerical results for $\nu_{ei}(\omega)$ have been shown for dense aluminum covering a broad temperature range, especially the region of intermediate temperatures that cannot be described by the high- and low-temperature asymptotes. Ionic correlations affect the electron-ion collision frequency quantitatively at not too high temperatures and small laser frequencies (corresponding to long wavelengths). On the other hand, our results show a significant field influence for small laser frequencies and moderate to low temperatures. However, the linear response description turns out to be valid up to rather high fields, especially for short-wavelength lasers.

Corresponding to the discussion of approximations used in Sec. III, the following extensions of the approach have to be investigated in the future: (i) using HNC simulation results for the ionic structure factor also for the (experimentally more realistic) case of a two-temperature plasma with $T_i \ll T_e$, (ii) including the dielectric function of the electrons ε_{ee} in an approximation beyond RPA (e.g., the Gould-DeWitt scheme), and (iii) including the electron-ion interaction taking into account the finite extension and the internal charge structure of the ion, e.g., using a pseudopotential. Furthermore, the connection to the electron-phonon interaction in the solid state has to be improved in the temperature region where both concepts overlap in order to describe the low-temperature range, too.

To summarize, our approach to collisional absorption in laser fields provides an efficient tool for studies of warm dense matter. It can also be used as input in hydrodynamic simulations of solid density matter at arbitrary temperatures.

ACKNOWLEDGMENTS

The authors wish to thank D. Kremp (Rostock), M. Schlanges (Greifswald), Th. Tschentscher (DESY Hamburg), E. Förster (Jena), A. Höll (Rostock), and V. Bezkrovniy (Rostock) for fruitful and stimulating discussions. We thank V. Bezkrovniy (Rostock) for providing us with the HNC data shown in Fig. 2. This work was supported by the Helmholtz-Gemeinschaft (Virtual Institute VH-VI-104) and by the Deutsche Forschungsgemeinschaft (SFB 652).

[1] M. D. Perry and G. Mourou, Science **264**, 917 (1994).
[2] J. D. Lindl *et al.*, Phys. Plasmas **11**, 340 (2004).
[3] L. Bergé *et al.*, Phys. Rev. Lett. **92**, 225002 (2004).
[4] LCLS Design Study Group Collaboration, J. Arthur *et al.*, *Linac Coherent Light Sources (LCLS) Design Study Report* SLAC-R-0521 (1998).
[5] *TESLA Technical Design Report, Part V: The X-ray Free Electron Laser*, edited by G. Materlik and T. Tschentscher (DESY Hamburg, Germany, 2001), DESY Report 2001-011.
[6] T. Tschentscher and S. Toleikis, Eur. Phys. J. D **36**, 193 (2005).
[7] A. Krenz and J. Meyer-ter-Vehn, Eur. Phys. J. D **36**, 199 (2005).
[8] H. Wabnitz *et al.*, Nature (London) **420**, 482 (2002).
[9] S. H. Glenzer *et al.*, Phys. Rev. Lett. **90**, 175002 (2003).
[10] G. Gregori, S. H. Glenzer, W. Rozmus, R. W. Lee, and O. L. Landen, Phys. Rev. E **67**, 026412 (2003).
[11] A. Höll, R. Redmer, G. Röpke, and H. Reinholz, Eur. Phys. J. D **29**, 159 (2004).
[12] R. Redmer, H. Reinholz, G. Röpke, R. Thiele, and A. Höll, IEEE Trans. Plasma Sci. **33**, 77 (2005).
[13] K. Eidmann, J. Meyer-ter-Vehn, T. Schlegel, and S. Hüller, Phys. Rev. E **62**, 1202 (2000).
[14] D. Fisher, M. Fraenkel, Z. Henis, E. Moshe, and S. Eliezer,

Phys. Rev. E **65**, 016409 (2001).
[15] Th. Bornath, M. Schlanges, P. Hilse, and D. Kremp, J. Phys. A **36**, 5941 (2003).
[16] D. Kremp, T. Bornath, M. Bonitz, D. Semkat, and M. Schlanges, Contrib. Plasma Phys. **45**, 396 (2005).
[17] P. Hilse, M. Schlanges, Th. Bornath, and D. Kremp, Phys. Rev. E **71**, 056408 (2005).
[18] S. Pfalzner and P. Gibbon, Phys. Rev. E **57**, 4698 (1998).
[19] D. Semkat, D. Kremp, and M. Bonitz, J. Phys.: Conf. Ser. **11**, 25 (2005).
[20] D. Kremp, Th. Bornath, M. Bonitz, and M. Schlanges, Phys. Rev. E **60**, 4725 (1999).
[21] Th. Bornath, M. Schlanges, P. Hilse, and D. Kremp, in *Nonequilibrium Physics at Short Time Scales: Formation of Correlations*, edited by K. Morawetz (Springer-Verlag, Berlin, 2004), pp. 153–172.
[22] D. Kremp, M. Schlanges, and W.-D. Kraeft, *Quantum Statistics of Nonideal Plasmas* (Springer, Berlin, 2005).
[23] Th. Bornath, D. Kremp, and M. Schlanges (unpublished).
[24] G. Bekefi, *Radiation Processes in Plasmas* (Wiley, New York 1966).
[25] H. Reinholz, R. Redmer, G. Röpke, and A. Wierling, Phys. Rev. E **62**, 5648 (2000).
[26] C. Oberman, A. Ron, and J. Dawson, Phys. Fluids **5**, 1514 (1962); J. M. Dawson and C. Oberman, *ibid.* **6**, 394 (1963).
[27] V. P. Silin, Zh. Eksp. Teor. Fiz. **47**, 2254 (1964) [Sov. Phys. JETP **20**, 1510 (1965)].
[28] M. Schlanges, P. Hilse, Th. Bornath, and D. Kremp, in *Progress in Nonequilibrium Green's Functions II*, edited by M. Bonitz and D. Semkat (World Scientific, Singapore, 2003), pp. 50–65.
[29] H. Haberland, M. Bonitz, and D. Kremp, Phys. Rev. E **64**, 026405 (2001).
[30] Th. Bornath, M. Schlanges, P. Hilse, and D. Kremp, Phys. Rev. E **64**, 026414 (2001).
[31] *Handbook of Chemistry and Physics*, 76th ed. (CRC Press, Boca Raton, FL, 1995).
[32] K. Widmann *et al.*, Phys. Rev. Lett. **92**, 125002 (2004).
[33] P. Audebert *et al.*, Phys. Rev. Lett. **94**, 025004 (2005).
[34] D. O. Gericke, M. S. Murillo, and M. Schlanges, Phys. Rev. E **65**, 036418 (2002).
[35] S. Mazevet, J. Clerouin, V. Recoules, P. M. Anglade, and G. Zerah, Phys. Rev. Lett. **95**, 085002 (2005).
[36] H. J. Kull and L. Plagne, Phys. Plasmas **8**, 5244 (2001).
[37] D. G. Yakovlev and V. A. Urpin, Astron. Zh. **57**, 526 (1980) [Sov. Astron. **24**, 303 (1980)].
[38] V. F. Gantmakher and Y. B. Levinson, *Carrier Scattering in Metals and Semiconductors* (North-Holland, Amsterdam, 1987).
[39] V. E. Zinov'ev, *Handbook of Thermophysical Properties of Metals at High Temperatures* (Nova Science, New York, 1996).